Appl. Environ. Microbiol. doi:10.1128/AEM.01538-15

Changes of microbial biofilm communities during colonization of sewer systems

Auguet O[1], Pijuan M.[1], Batista J. [1], Borrego C.M.[1,2,*], Gutierrez O.[1]

[1] Catalan Institute for Water Research (ICRA), Scientific and Technological Park UdG, Girona, Spain.

Email: oauguet@icra.cat, mpijuan@icra.cat, cborrego@icra.cat , ogutierrez@icra.cat

[2] Group of Molecular Microbial Ecology, Institute of Aquatic Ecology, University of Girona, Girona, Spain. Email: carles.borrego@udg.cat

[*] *Corresponding author*: cborrego@icra.cat, Phone: +34 972 183380; FAX: +34 972 183248

ABSTRACT

Coexistence of sulfate-reducing bacteria (SRB) and methanogenic archaea (MA) in anaerobic biofilms developed in sewer inner pipe surfaces favours the accumulation of sulfide (H_2S) and methane (CH_4) as metabolic end products, causing severe impacts on sewerage systems. In this study we investigated the time-course of H_2S and CH_4 production and emission rates during different stages of biofilm development in relation to changes in the composition of microbial biofilm communities. The study was carried out in a laboratory sewer pilot plant that mimics a full-scale anaerobic rising sewer using a combination of process data and molecular techniques (*e.g.* qPCR, DGGE and 16S rRNA gene pyrotag sequencing). After two weeks of biofilm growth, H_2S emission was notably high (290.7±72.3 mg S-H_2S l^{-1} day^{-1}) whereas emissions of CH_4 remained low (17.9±15.9 mg COD-CH_4 l^{-1} day^{-1}). This contrasting trend coincided with a stable SRB community and an archaeal community solely composed of methanogens derived from the human gut (*i.e. Methanobrevibacter* and *Methanosphaera*). In turn, CH_4 emissions increased after one year of biofilm growth (327.6±16.6 mg COD-CH_4 l^{-1} day^{-1}) coinciding with the replacement of methanogenic colonizers by species more adapted to sewer conditions (*i.e. Methanosaeta* spp.). Our study provides data that confirm the capacity of our laboratory experimental system to mimic the functioning of full-scale sewers both microbiologically and operationally in terms of sulfide and methane production, gaining insight on the complex dynamics of key microbial groups during biofilm development.

INTRODUCTION

Wastewater collection systems, or sewers, consist of an underground network of physical structures-installations composed of pipelines, pumping stations, manholes and channels that convey wastewaters from its source to the discharge point, usually a wastewater treatment plant (WWTP). Sewer systems thus prevent direct contact of urban population to faecal material and potential microbial pathogens, greatly reducing the spread of infectious diseases. Sewers have traditionally only been considered as hydraulic transport systems for sewage although they are in fact "reactors" where complex physicochemical and microbial processes take place. Wastewater microorganisms are diverse and abundant and they are exposed to a wide range of both inorganic and organic substrates as well as changing conditions along their transport through sewers (1). In this regard, wastewater transport through the pipes facilitates the formation of microbial biofilms that grow attached to the inner surface of sewer pipes (2). Different factors such as high surface area, low flow velocity near pipe walls and nutrient availability may favour microbial colonization of pipe surfaces and biofilm growth. Formation of fully functional biofilms occurs in different steps, from surface conditioning, adhesion of microbial "colonizers", initial growth and glycocalyx formation followed by secondary colonization and growth (3).

Anaerobic conditions in sewer pipes favour the accumulation of both sulfide (H_2S) and methane (CH_4) as end products of different microbial metabolisms, *i.e.* anaerobic respiration of organic matter by sulfate-reducing bacteria (SRB) and methanogenic archaea (MA), respectively. Both compounds have detrimental effects on the sewer system with different consequences on both the installation and its surroundings (2). Accumulation of H_2S in the sewer atmosphere causes malodour in the whole system,

health hazards due to the well-known toxicity of H_2S, and corrosion of both the inner surface of pipes and the inlet zones of WWTPs (4, 5). H_2S accumulation also impacts the structural integrity of the sewerage by microbial-mediated corrosion processes, which severely affect the performance and cost of downstream processes at the WWTPs (2, 6). Remediation or replacement of corroded pipes require high economic investment for large systems, ranging from several hundreds to several thousands € per m depending on pipe diameter and location depth (7). On the other hand, build-up of CH_4 in sewers results from the activity of MA that colonize inner pipe surfaces and develop within the biofilm matrix under strict anaerobic conditions (8–10). In addition of being explosive at low concentrations, CH_4 is a major greenhouse gas with a lifespan of about 12 years and a global warming potential of roughly 21–23 times higher than that of carbon dioxide (11). Recent reports suggest that CH_4 emissions from sewers contribute significantly to the total greenhouse gas footprint of wastewater systems (12, 13). Accordingly, different mitigation strategies have been used to reduce H_2S and CH_4 production in sewers (14–24).

Although competition between SRB and MA has been reported in some environments such as freshwaters (25), sediments (25) and WWTPs (26), CH_4 production in sewers containing high sulfate concentrations was first detected by Guisasola and co-workers (8). Assuming that SRB and MA may compete for the same substrates (*e.g.* complex organic matter, acetate, hydrogen) their co-occurrence in sewer systems is probably the rule rather than the exception, especially considering the large amount of organic matter in wastewater and the prevalence of anaerobic conditions in many sections of the sewer networks. In biofilms, this co-existence may be explained by mass transfer processes of required substrates (*e.g.* sulfate and organic matter) into the biofilm matrix, which result in a physicochemical stratification along its thickness. Very

82 recently, Sun and co-workers (10) investigated the stratification pattern of SRB and MA
83 in sewer biofilms thicker than 800 µm, locating the former closer to the biofilm surface
84 and locating the latter in greater abundance at deeper, highly anaerobic layers.

85 Despite these findings, little information is available on the colonization dynamics
86 and activity of SRB and MA relating to biofilm development in sewer systems.
87 Particularly, processes behind early biofilm colonisation by SRB and MA in sewer
88 pipes are still not fully understood. In this regard, a better understanding of how these
89 processes take place and how they affect H_2S and CH_4 production rates during biofilm
90 development is necessary to design effective biofilm-control strategies for the
91 commissioning of sewers. This information could be crucial to the development and
92 application of optional control-methods to reduce odour, corrosion and global warming
93 issues generated by sewer biofilms.

94 The aim of this study was to investigate the initial stages of microbial biofilm
95 development in sewer systems with a special focus on the interactions between SRB and
96 MA. Biological activities and phylogenetic community structure during the colonisation
97 phase were investigated using a combination of molecular techniques (DGGE, qPCR
98 and massive parallel sequencing of 16S rRNA genes from target groups) and process
99 data (H_2S and CH_4 production). The work was carried out using a laboratory sewer pilot
100 plant fed with wastewater that reproduced a full-scale anaerobic pressured sewer.
101 Microbial community composition was compared with biofilm from a full-scale sewer
102 to validate the data obtained from our laboratory experiments.

103 ## MATERIALS AND METHODS

104 **Anaerobic sewer biofilm reactor system.** The study was carried out in a specially
105 designed pilot system previously validated, the SCORe-CT method (27), that mimics

106 H_2S and CH_4 production capacity of full-scale rising main sewers by reproducing its
107 main characteristics including: *i)* hydraulic features: hydraulic retention times (HRT),
108 turbulence and Area-to-Volume ratio (A/V), and *ii)* wastewater characteristics
109 associated with real sewage. The laboratory system consisted of 3 airtight reactors (R1,
110 R2, R3) each of them mimicking a section of an anaerobic sewer pipe (Fig. S1). Each
111 reactor had a volume of 0.75 l, 80 mm of diameter and a height of 149 mm. The system
112 was fed with fresh sewage (domestic fresh sewage collected in the upstream sections of
113 the sewer network in the municipality of Girona, close to its source in households) by a
114 peristaltic pump (Masterflex model 7518-10). Sewage was collected on a weekly basis
115 and kept at 4ºC to minimize variation in its composition. Wastewater contained
116 26.5±2.6 mg $S\text{-}SO_4^{2-}$ l^{-1} and 0.1±0.1 mg $COD\text{-}CH_4$ l^{-1}. Volatile Fatty Acids (VFA) and
117 soluble and total Chemical Oxygen Demand (COD) concentration were 42.3±8.3 mg
118 COD-VFA l^{-1}, 325.8±40.8 mg soluble COD l^{-1} and 672±93.2 mg total COD l^{-1}
119 respectively. Sewage was heated to 20ºC before entering the reactors. Magnetic stirrers
120 (Heidolph Mr Hei-MixS) were used to ensure homogeneous conditions and to produce a
121 shear within the reactors. Wastewater was pumped 15 times a day in uneven periods
122 (between 1 and 3 hours). During these intervals, wastewater was transferred from the
123 storage tank to R1, then from R1 to R2 and, finally, from R2 to R3 in order to simulate
124 the HRT pattern observed in a full-scale rising main used as a reference sewer pipe, the
125 Radin collector (42.101843 N 3.131631 E, L'Escala municipality, Spain). The Radin
126 anaerobic pipe is 2,930 m long and has 0.5 m of diameter with an HRT between 3–7
127 hours.

128 Plastic carriers (Anox Kaldnes, Norway) of 1 cm diameter were clustered on three
129 stainless steel rods inside each reactor to increase biofilm growth surface area and to
130 provide easily extractable biofilm samples. Taking into consideration reactor wall and

carriers, the total biofilm growth area in each reactor was 0.05 m^2 (Area/Volume ratio of 65 m^2 m^{-3}). The system was operated continuously for 48 weeks. Colonization period was monitored during the first 12 weeks after start-up of the system. In addition, characterization of mature biofilms was undertaken during the 12th month after start-up. Microbial community composition of mature biofilms was compared to biofilm extracted from the upstream reference section of the Radin sewer pipe. Biofilm sample from the full-scale sewer pipe was obtained from a sewer air scour valve that was constantly in contact with the flowing wastewater. The valve was disassembled and the biofilm grown on its surface was scrapped using a sterile spatula and collected in a sterile Falcon tube containing 5 ml of Phosphate Buffered Saline (PBS, NaCl 137 mM; KCl 2.7 mM; Na_2HPO_4 10 mM; KH_2PO_4 1.8 mM), into which the collected biomass was resuspended. The sample tube was maintained at 4ºC in a portable icebox until arrival to the laboratory (1 hour after collection) where it was immediately frozen at –20ºC until DNA extraction.

H_2S generation, CH_4 production and VFA production/consumption in the laboratory system were monitored as the wastewater was transported through the system. Liquid phase sampling from R3 and off-line chemical analyses were done weekly during Normal Functioning tests (NF) for the determination of sulfur species (sulfate, sulfide, sulfite and thiosulfate), CH_4, COD and VFA. Sampling hours covered all of the HRT range (3h–7h). Also, 10 batch tests (BT) were performed to monitor H_2S and CH_4 production by biofilms. Batch tests were carried out once every 1–2 weeks. During BT the continuous operation of the reactors was stopped. The feed pump was activated for 10 minutes to ensure each reactor was filled with fresh sewage. After that, the feed was stopped and liquid samples were withdrawn every hour for a 3-hour period using a 10 ml syringe connected through a sampling port fitted with a valve and Tygon tubing.

156 Samples were analysed for sulfur species, CH_4, VFA and COD as described below.
157 Using linear regression, H_2S and CH_4 production rates were calculated from the
158 sampling-point data. A special 6-hour batch test was run in order to investigate changes
159 of methane production depending on sulfate presence in R1 and R3. Samples were
160 analyzed every hour over a 3-hour period for sulfur species, and every hour for a 6-hour
161 period for methane in order to determined changes of methane production when sulfate
162 was totally reduced to sulfide.

163 Daily H_2S and CH_4 emissions (calculated from NF test data) were also determined
164 after one year of biofilm development to detect changes in activity between early and
165 mature stages of biofilm development in the system.

166 **Chemical analysis.** Dissolved sulfide was measured continuously in R1 and R3
167 using an UV–VIS spectrometer probe s::can spectro::lyser (Messtechnik, GmbH,
168 Austria) (28). For the analysis of dissolved sulfur species, 1.5 ml of wastewater was
169 filtered through disposable Millipore filter units (0.22 µm pore size) and added to 0.5 ml
170 preserving solution antioxidant buffer (SAOB) (29). Samples were analysed within 24 h
171 in an ion chromatograph (IC) with UV and conductivity detector (Dionex ICS-5000).
172 VFA were measured by gas chromatography (Thermofisher Scientific, coupled with
173 FID detector). For CH_4 samples, 5 ml of sewage were filtered through disposable
174 Millipore filter units (0.45 µm pore size) and injected into vacuumed glass tubes, with
175 the help of a hypodermic needle attached to plastic syringe. After reaching liquid-gas
176 equilibrium inside the tubes, the samples were analysed by gas chromatography
177 (Thermofisher Scientific, coupled with FID detector). COD analyses were performed
178 using a standard photometric test kit with commercially available reagent (LCK 114,
179 Hach Lang). Absorbance readings were obtained using LCK 314 cuvette test in a

DR2800 Hach Langue spectrometer. During start up, Anox Kaldnes plastic carriers were regularly withdrawn to quantify changes in biomass content as a result of microbial biofilm formation. Biomass attached to each carrier was suspended in MilliQ water by vortexing (IKA, genius 3) until complete detachment (≈ 2 min). Concentration of total and volatile suspended solids (TSS, VSS) was analysed using standard methods 2510D (30). Biomass content was referred to carrier surface using volatile suspended solids values.

DNA extraction. DNA was extracted from biofilm biomass collected in reactor R1 and from sewage at different week intervals during the study period. Biomass attached to each carrier was suspended in 5 ml 1× PBS by vortexing (IKA, Genius-3). Suspended biomass from carriers and samples of wastewater (45 ml) were centrifuged at 11,000 rpm for 5 min at 25ºC in an Eppendorf Centrifuge 5804R equipped with a F-34-6-38 rotor (Eppendorf, Hamburg, Germany). DNA was then extracted from pelleted biomass using the FastDNA Spin Kit for Soil (MP Biomedicals, Santa Ana, CA, USA) according to manufacturer's instructions. Genomic DNA concentrations of biofilm samples were measured using a Nanodrop 2000 spectrophotometer (Thermo Scientific, Wilmington, DE, USA).

PCR amplification and 16S rRNA gene fingerprinting. The microbial composition of biofilms formed on carrier surfaces was studied by combining specific amplification of 16S rRNA gene fragments and fingerprinting by denaturing gradient gel electrophoresis (DGGE) (31). Bacterial and archaeal 16S rRNA gene fragments were amplified from DNA extracts using primer pairs 357F-GC/907R (32) and 109(T)F/515R-GC (33), respectively. PCR amplifications (final volume of 50 µl) contained 10 µl of Buffer $MgCl_2$ (15 mM), 1 µl of dNTPs (10 mM), 2 µl BSA, 1 µl of

each primer (10µM), 0.25 µl of Taq Polymerase and 2 µl of DNA sample. DNA extracts were diluted with sterile MQ water to a final concentration of 10–50 ng μl^{-1} to avoid inhibition of amplification reactions. Sequences of the different primer pairs used during the study and PCR conditions are summarized in Supplementary Tables S1 and S2, respectively.

DGGE analyses were run in an INGENY phorU-2 DGGE system (Ingeny International BV, Netherlands). Samples were loaded onto 6% polyacrylamide gels and run with 1× TAE buffer using a 30–70% (bacterial 16S rRNA) and a 30–50% (archaeal 16S rRNA) linear denaturing gradients of urea-formamide (100% denaturant agent contained 7M urea and 40% deionized formamide). A molecular ladder composed by a mixture of known SSU rRNA gene fragments was loaded in all gels to allow inter-gel comparison of band migration. Electrophoreses were run overnight at 60°C and at a constant voltage of 120 V. After electrophoresis, gels were stained for 30 min with 1× SYBR Gold nucleic acid stain (Molecular Probes Inc.) in 1× TAE buffer, rinsed and visualized under UV radiation. DGGE fingerprints were analyzed using GelCompar II (Applied Maths, Belgium). For sample comparison, a presence-absence matrix was used to calculate similarities between patterns and statistical analysis based on hierarchical cluster analysis was performed with the Dice distance and the UPGMA grouping algorithm.

DNA from excised bands of wastewater samples was eluted as previously described (34). DNA was then amplified using the same primer pairs (without GC clamp) and PCR conditions as before but sizing down the number of PCR cycles up to 20. PCR products were directly sent for sequencing on both strands to Genoscreen (Lille, France). Sequences were checked for chimeras using Uchime (35), aligned using

Applied and Environmental Microbiology

BioEdit (36), manually curated and then compared for the closest relatives in NCBI sequence database (http://www.ncbi.nlm.nih.gov/blast/) using the Basic Local Alignment Search Tool (BLAST) (37). Bacterial and archaeal 16S rRNA gene sequences obtained in DGGE fingerprintings were deposited in GenBank under accession numbers KR080151- KR080166.

Real-time quantitative PCR. Real-time quantitative PCR (qPCR) assays were used to quantify gene copies of bacterial and archaeal 16S rRNA and *dsrA* functional genes. All qPCR reactions were run in a Stratagene MX3005P (Agilent Technologies). For all tests, qPCR standards contained a known number of target 16S rRNA genes. qPCR for bacterial genes contained 15 µl Brilliant III Ultra Fast SYBR Green qPCR Master Mix (Agilent Technologies), 400 nM each of forward (1048F) and reverse (1194R) primers (38), 1 µl of template and adjusted to a final volume of 30 µl with MB Grade sterile water. DNA sample stocks were diluted with water to a final concentration of 10-20 ng μl^{-1}. qPCR for archaeal 16S rRNA genes were carried out using the same conditions as for bacteria but using forward primer 806F (39) and reverse primer 915R (40) and reducing the number of cycles to 35. Quantification of SRB was based on the dissimilatory sulfate reductase subunit A (*dsrA*) gene according to Ben-Dov et al. (2007) (41). Primer sequences, reaction temperatures, R^2 values and amplification efficiencies for each qPCR reaction are compiled in supplementary tables S1 and S3. All qPCR analyses carried out followed the MIQE rules for quantitative PCR analyses (42) and all essential information has been included in this section.

Pyrosequencing and phylogenetic analyses of microbial diversity. DNA extracts from biofilms at early stages (weeks 1, 5 and 13), mature biofilms (one-year old), and from full-scale sewers were analysed through tag-encoded FLX-Titanium amplicon

pyrosequencing at the Research and Testing Laboratory (Lubbock, TX, USA). Briefly, genomic DNA from biofilm samples was used as a template in PCR reactions using universal bacterial (28F/519R) (33) and archaeal (341F/958R) (43, 44) primer combinations complemented with 454-adapters and sample-specific barcodes. Raw sequence datasets were pre-processed at RTL facilities to reduce noise and sequencing artefacts as previously described (45). Demultiplexing according to sample barcodes, sequence quality assessments, chimera detection and downstream phylogenetic analyses were conducted in MOTHUR (46). Bacterial and archaeal curated sequence datasets were then aligned in MOTHUR using the bacterial and archaeal SILVA reference alignments, respectively, available at the MOTHUR website (http://www.mothur.org). Taxonomic classification of bacterial sequences was carried out using the RDP taxonomy reference database with a cutoff value of 80% for valid assignments. Classification of archaeal sequences was carried out using the SILVA reference database and taxonomy files using the same cutoff as for bacteria (80%). Operational Taxonomic Units (OTUs, 97% cutoff) and representative sequences of each OTU were delineated and taxonomically assigned using MOTHUR. For community analysis, the number of sequences in each sample was normalized using a randomly selected subset of 1,500 sequences (for Bacteria) and 6,000 sequences (for Archaea) from each sample to standardize the sequencing effort across samples and minimize any bias due to a different number of total sequences. These normalized sequence datasets were then used in MOTHUR to calculate α-diversity indicators of richness (Chao1) and diversity (Shannon) and to calculate community similarity among sites (β-diversity) based on weighted UniFrac distance (47). Non-metric multidimensional scaling (nMDS) analysis was performed on the UniFrac similarity matrices to visualize patterns of community composition. Relative abundance of the most populated OTUs (OTUs with relative abundances ≥4%

277 of total sequences in at least one sample) across samples was visualized as bubble plots
278 using bubble.pl (http:// www.cmde.science.ubc.ca/hallam/bubble.php). Pyrosequencing
279 data of this study have been deposited in the NCBI database via the Biosample
280 Submission Portal (http://www.ncbi.nlm.nih.gov/biosample/) under accession number
281 PRJNA279227.

282 After taxonomic classification of bacteria, sequences affiliated to class
283 *Deltaproteobacteria* were selected and further grouped into 149 OTUs (97% cutoff).
284 Representative sequences of each deltaproteobacterial OTU were delineated and
285 assigned using MOTHUR and then compared for the closest cultured relative using
286 BLAST. Phylogenetic trees were constructed in MEGA 5 (48) using representative
287 sequences of abundant OTUs, defined as those having a relative abundance ≥ 4% of
288 total deltaproteobacterial and archaeal sequences in at least one sample and closest
289 cultured representative sequences.

290 **Statistical analyses.** Statistical analyses were carried out using SPSS (version 15.0;
291 SPSS, Chicago, IL, U.S.A.). Normality of data was assessed by the Kolmogorov-
292 Smirnov test for values obtained during batch test and inlet wastewater (sulfate and
293 sulfur balance). Correlation between sulfate concentration in wastewater and sulfate
294 reduction rates was assessed by the Pearson test.

295 ## RESULTS

296 **Differences in sulfide and methane production/emission between young and**
297 **mature biofilms in laboratory and full-scale sewer systems.** Changes in microbial
298 biomass were continuously monitored for 12 weeks after the beginning of the
299 experiment to assess biofilm formation within bioreactors (Fig. 1A). The initial biofilm

300 growth was detected after stabilization of biomass content in the range between 2.1–3.5
301 mg VSS cm^{-2}.

302 The daily profile of H_2S measured using an UV–VIS spectrometer probe s::can
303 spectro::lyser showed a gradual increase of H_2S production during the first 12 weeks of
304 biofilm development in R1 and R3 (Fig. S2). The higher H_2S production rate
305 determined in R1 compared to R3 was probably related to the low sulfate in the
306 wastewater arriving at R3. H_2S and CH_4 production rates were calculated for the same
307 time period to assess the activity of recently formed biofilms. Figure 1B shows the H_2S
308 production capacity within reactors in batch test experiments. H_2S production increased
309 immediately after the start-up of the system. After the second week of operation, the
310 capacity of the biofilm to produce H_2S stabilized between 3.5–7.7 mg S-H_2S l^{-1} h^{-1}.
311 Sulfate reduction rates were between 3.2–7.7 mg S-SO_4^{2-} l^{-1} h^{-1}, which were positively
312 related to H_2S production rates in each reactor (Fig. S3). Differences in H_2S production
313 showed a good correlation with the sulfate concentration in inlet wastewater (Pearson
314 correlation index R=0.881, p=0.02). Interestingly, from week 8 to week 12, H_2S
315 production in reactor R1 was higher than in R2 and R3. Regarding CH_4 production, low
316 rates were detected in all reactors during these early stages of development (0.08±0.11,
317 0.12±0.16 and 0.16±0.16 mg COD-CH_4 l^{-1} h^{-1} in R1, R2 and R3, respectively).

318 Sulfide emission was measured weekly for 24 h to evaluate the impact of SRB
319 activity in the system, mimicking an accurate representation of the full-scale sewer
320 conditions. After the second week of operation, H_2S emission ranged between 195.7 and
321 388.8 mg S-H_2S l^{-1} day^{-1} (Fig. S4A), representing 78.6%±14.0% of the inlet sulfate.
322 Therefore, some SO_4^{2-} was still present in the effluent wastewater (75.3±33.0 mg S-
323 SO_4^{2-} l^{-1} day^{-1}) because not all sulfate in the influent wastewater was reduced within the

system. On the other hand, CH_4 emissions were very low (between 0 and 8.7 mg COD-CH_4 l^{-1} day^{-1}) for the first 6 weeks (Fig. S4B) but increased to values as high as 44.5 mg COD-CH_4 l^{-1} day^{-1} from week 8 to week 12.

A 6-hour batch test experiment was carried out during week 14 (Fig S5) to assess if CH_4 production was limited by the presence of sulfate. For the first 4 h, the CH_4 production rate in R3 was twice that in R1 (R1=0.37 and R3=0.88 mg COD-CH_4 l^{-1} h^{-1}). Remarkably, CH_4 production increased after 4 hours of testing (R1=1.06 and R3=2.07 mg COD-CH_4 l^{-1} h^{-1}) coinciding with the reduction of all sulfate available.

High variability of VFA production rates was observed due to the simultaneous production and consumption of these compounds during batch test experiments (Fig S6A). Nevertheless, VFA production rates were remarkably low for the first two weeks of biofilm development. Furthermore, the concentration of VFA exiting the system was higher in comparison to values measured in inlet wastewater (Fig S6B).

Comparison of H_2S and CH_4 emissions measured after one year of biofilm development with those calculated during the first three months of operation in the laboratory suggested similar activity of SRB but clear differences in methanogenesis. After one year of growth, emission of H_2S by laboratory biofilms were slightly different (204.7±14.6 mg S-H_2S l^{-1} day^{-1}) from that measured at the initial stage (316.5±61.0 mg S-H_2S l^{-1} day^{-1}). This discrepancy may have been caused by differences in sulfate concentration of the inlet wastewater between the two periods (26.7±2.5 mg S l^{-1} and 16.0±1.0 mg S l^{-1} during the first weeks and after one year, respectively). Regardless of these differences in absolute values, mature biofilms performed better when these concentrations were compared in relative terms (around 80% and 100% of SO_4^{2-} reduced to H_2S during initial weeks and after one year of operation, respectively). In

348 turn, CH_4 emissions largely increased after one year of biofilm growth (from 17.9±15.9
349 mg COD-CH_4 l^{-1} day^{-1} to 327.6±16.6 mg COD-CH_4 l^{-1} day^{-1}).

350 To determine if the high production of H_2S and CH_4 in mature biofilms under
351 laboratory conditions were similar to emissions of these compounds under natural
352 conditions (*e.g.* full-scale sewers) we calculated the daily production of both
353 compounds in both systems. Whereas full-scale sewers discharged 4.56 g S-H_2S day^{-1}
354 m^{-2} laboratory systems produced 1.58 g S-H_2S day^{-1} m^{-2}. Similar values were obtained
355 for CH_4 production; whereas the full-scale sewer produced 4.24 g COD-CH_4 day^{-1} m^{-2}
356 laboratory systems emitted 1.65 g COD-CH_4 day^{-1} m^{-2}.

357 **Changes in the composition of microbial communities during biofilm**
358 **development.** DGGE fingerprints showed compositional differences over the study
359 period between the bacterial community in the inlet wastewater and that of biofilms
360 grew in R1 (Fig. 2A). Even though several bands were consistently detected at different
361 time intervals, the variation in the banding pattern suggested changes in the composition
362 of bacterial communities during biofilm development. Hierarchical clustering of
363 samples according to Dice similarity index clearly segregated wastewater samples from
364 laboratory biofilms. Moreover, biofilm samples clustered according to date of collection
365 (*e.g.* developmental stage). Less variation between wastewater and biofilm samples was
366 observed for archaeal communities although similar clustering of biofilm samples
367 according to date was distinguished (Fig. 2B). A total of 16 of the 23 excised bands (9
368 and 7 bands from the bacterial and archaeal wastewater communities, respectively) (Fig.
369 S7) yielded good quality sequences. Differences in bacterial closest relatives identified
370 and band patterns showed high variability of wastewater bacterial communities. On the

other hand, closest relatives of the identified archaea were less diverse, belonging to *Methanobrevibacter smithii* and *Methanosphaera stadtmanae* (Table S4).

Variations in bacterial and archaeal abundance in R1 biofilms were assessed by qPCR during the study period devoted to monitoring biofilm development. Although bacterial 16S rRNA gene copies were always higher than archaeal 16S rRNA copies, both genes showed similar trends in increase of copies for the first two weeks of growth followed by a steady state that suggested a balanced composition of biofilm communities for the rest of the study period (Fig. S8). Remarkably, *dsrA* gene abundance showed a similar time course as bacterial 16S rRNA genes (Fig. S8) suggesting a similar growth dynamics of SRB for the first two weeks of experiment.

Composition of microbial communities from R1 and full-scale sewer biofilms were assessed by massively parallel sequencing to determine whether or not H_2S and CH_4 production rates measured over time were related to compositional changes of bacterial and archaeal biofilm communities. Bacterial and archaeal 16S rRNA gene libraries were constructed using pyrotags from different samples collected during the study period (Week 1, Week 5, Week 13, One year and full-scale Sewer). Relative contribution of bacterial phyla changed during biofilm development (Fig. 3A). Furthermore, the composition of the bacterial community in one-year-old biofilms was clearly different from that of the full-scale sewer system (Fig. 3A). Sequences affiliated to bacterial classes *Bacilli*, *Fusobacteria* and *Gammaproteobacteria* progressively decreased during biofilm maturation. It is noteworthy that no sequences affiliated to these classes were identified in the bacterial community from the full-scale sewer biofilm. In turn, sequences affiliated to class *Betaproteobacteria* were prevalent in the full-scale sewer biofilm and in R1 samples collected at the first stages of biofilm development (20–26%

of total sequences) but they showed less representativeness after one year of operation (4.9% of total sequences). On the other hand, sequences affiliated to classes *Synergistia* and *Deltaproteobacteria* increased during biofilm colonization, reaching similar relative abundances as those found in full-scale sewer biofilm. Concerning archaeal communities, no archaea other than methanogens were identified in pyrotag libraries from biofilms samples. Specifically, archaeal sequences affiliated to three main genera: *Methanosphaera, Methanobrevibacter* and *Methanosaeta*. Whereas sequences affiliated to *Methanosphaera* (relative abundances ranging from 10 to 23%) and *Methanobrevibacter* (76–86%) were prevalent during the first weeks of biofilm development (Fig. 3B), the archaeal community in one-year-old biofilms was mainly dominated by sequences affiliated to genus *Methanosaeta,* which were also prevalent in the biofilm collected from the full-scale sewer (Fig. 3B).

Grouping sequences into OTUs (97% cutoff) resulted in 1,283 and 137 OTUs for Bacteria and Archaea, respectively (Table S5). OTU delineation allowed us to identify potentially those OTUs (*i.e.* species) that may make a relevant contribution in the development and activity of sulfidogenic and methanogenic biofilms. Because of the high diversity of the sample and nutrient availability in the system, OTUs were considered relevant in terms of abundance if their relative abundance was ≥4% in at least one sample. Whereas the relative abundance of some OTUs increased only at the end of the incubation period (OTU-B1, -B6 and -B7), that of others clearly decreased during this time (OTU-B3, -B8, -B10, -B12, and -B20) (Fig. 4A). One of the most prevalent OTUs in early stages of biofilm development (OTU-B3, >10% of total sequences) showed a 100% sequence identity to *Macellibacteroides fermentans*, a fermentative member of the *Porphyromonadaceae* (*Bacteroidetes*) (49). Other common OTUs identified during this period (*e.g.* OTU-B8 and OTU-B20) were rare in mature

and full-scale sewer biofilms. In turn, most prevalent OTUs in full-scale sewer biofilm were rare in the laboratory system with the exception of OTU-B1 (83% sequence identity to *Rikenella microfusus* strain Q-1, an obligate anaerobic fermentative microorganism) (50). The bacterial community in the biofilm collected from the full-scale sewer was composed mainly of microorganisms affiliated to class *Betaproteobacteria* (OTU-B2, -B14, and -B18), phyla *Synergistetes* (OTU-B4, -B5 and -B13) and *Chloroflexi* (OTU-B9) (Fig. 4A). Only OTU-B6 affiliated to class *Deltaproteobacteria* having a 99% sequence identity to *Desulfobacter postgatei* strain 2ac9.

In order to study the phylogenetic structure of the SRB community during biofilm development in more detail, sequences affiliated to class *Deltaproteobacteria,* which includes most of the sulfate reducers known to date, were retrieved and grouped into OTUs that were then used to construct a phylogenetic tree (Fig. S9A). Whereas abundant OTUs in the first weeks of incubation (OTU-D3 and OTU-D4) were phylogenetically related to *Desulfobulbus propionicus* strain DSM2032 (Fig. S10), the composition of the SRB community changed as biofilm developed. After one year of operation, the community was mainly dominated by OTU-D1 (36% of total deltaproteobacterial sequences) which showed a 99% sequence identity to *Desulfobacter postgatei* strain 2ac9 (Fig. S9A and Table S6). Although this OTU was also present in biofilms collected from a full-scale sewer, the deltaproteobacterial community in natural conditions was more diverse than that grown under laboratory conditions.

In turn, abundant archaeal OTUs (>4% of total sequences) were all affiliated to methanogenic lineages. Particularly, OTU-A1, which showed a 99% sequence

444 similarity to *Methanosaeta concilii,* was only detected in mature biofilms and in
445 biofilms from the full-scale sewer (Fig. 4B and Fig. S9B). In turn, OTU-A2 and OTU-
446 A3 were mainly detected during the first weeks of biofilm growth. Both OTUs had a
447 100% sequence identity to *Methanobrevibacter smithii* and *Methanosphaera*
448 *stadtmanae*, respectively. Finally, OTU-A4 (showing a 99% sequence similarity to
449 *Methanobrevibacter acididurans*) was detected at low relative abundances in all pyrotag
450 libraries analyzed.

451 Richness and diversity metrics calculated for the bacterial biofilm communities
452 increased during the experimental period (Table S7). However, the bacterial community
453 in the biofilm from the full-scale sewer was less rich and diverse than that from biofilms
454 under laboratory conditions. In turn, richness of archaeal community showed an
455 opposite trend, clearly decreasing during the 13 weeks of incubation but remained at
456 similar level in mature biofilms (Table S7). Despite these changes in richness, the
457 archaeal diversity remained fairly constant from the start-up to the end of the
458 monitoring period and decreased in mature biofilms. Moreover, both richness and
459 diversity of archaeal biofilm community in the full-scale in-sewer biofilm were higher
460 than the levels estimated from biofilms after one year of operation under laboratory
461 conditions.

462 To easily compare bacterial and archaeal biofilm communities, samples were
463 distributed in a nMDS 2D ordination space according to their similarity based on the
464 weighted UniFrac distance (Fig. S11). The ordination segregated biofilm samples
465 collected at early stages of development (Weeks 1, 5 and 13) from those collected in
466 mature stages from the lab-scale and from the biofilm samples from the full-scale
467 sewer. It is noteworthy that bacterial and archaeal communities in mature biofilms (*i.e.*

468 one year of incubation) were similar to those occurring in biofilms from full-scale
469 sewers.

470 DISCUSSION

471 **Sulfide and methane production rates during biofilm formation.** In this study we
472 investigated the association between H_2S and CH_4 production and the corresponding
473 biofilm development stage in a laboratory-scale anaerobic sewer pilot plant. H_2S
474 production rates suggested a fully adapted and functional SRB community after two
475 weeks of biofilm colonization. The low production of H_2S for the first two weeks may
476 have be a consequence of the low abundance of SRB in young biofilms after the
477 experimental set up (Fig. 4 and Fig. S8). In turn, the higher H_2S production in reactor
478 R1 compared to R2 and R3 may have resulted from the system design, considering that
479 the bioreactors were connected in series and that wastewater that entered R2 and R3
480 contained only trace amounts of sulfate because of its consumption in R1.

481 Methane production rates measured in batch tests were minimal for the first 12
482 weeks probably because reactors were filled with fresh wastewater (containing high
483 sulfate) just before the start-up of each batch test. The differences in CH_4 production
484 and emission rates might be a consequence of biofilm adaptation to each reactor
485 conditions, which mainly varied in terms of sulfate concentration and HRT. During
486 normal functioning, the low quantity of sulfate in the R1 effluent could have promoted
487 active methanogenesis in R2 and R3 whereas conditions in R1 (high sulfate and organic
488 matter), in turn, favoured SRB over MA (25, 51). Results from 6-hour batch test
489 experiment confirmed a stimulation of CH_4 production after 3–4 hours of wastewater
490 retention in the system (when sulfate was depleted), especially in R3 where sulfate
491 concentration was already low (Fig. S4). These results point to a spatial segregation of

492 microbial communities responsible for H_2S and CH_4 production along the length of the
493 anaerobic sewer although no direct evidences of this differential distribution were
494 obtained. Further work is then needed to validate if both composition and activity of
495 SRB and MA communities in sewer biofilms vary along length in full-scale sewer
496 systems.

497 **Sulfide and methane emissions by mature biofilms.** Comparison between H_2S
498 emissions from young and from mature biofilms showed a decrease as a consequence of
499 the lower amount of sulfate available in the influent wastewater. Notwithstanding this,
500 the relative amount of sulfate reduced to H_2S increased in mature biofilms (from ≈ 80%
501 to 100%). Concerning CH_4 emission, several factors could account for its increase in
502 mature biofilms (from 17.9±15.9 to 327.6±16.6 mg COD-CH_4 l^{-1} day^{-1}), namely: *i)* the
503 low sulfate concentration in the inlet wastewater after one year of experiment favouring
504 a higher methanogenic activity, *ii)* the high consumption rate of sulfate by SRB in
505 mature biofilms stimulating CH_4 production, or *iii)* a change in the composition of the
506 methanogenic community over time towards species more adapted to local conditions
507 resulting in a higher production of CH_4 .

508 **Compositional changes of microbial communities.** DGGE fingerprints showed
509 differences in the overall composition of bacterial and archaeal communities between
510 inlet wastewater and biofilm samples. Despite the inherent limitations of the PCR-
511 DGGE approach (52), similarity analysis of both bacterial and archaeal communities
512 based on DGGE band patterns grouped samples according to sampling date (*i.e.* stage of
513 biofilm development) showing that the structure of microbial biofilm communities
514 progressively adapted to local conditions in the system. The fact that both bacterial and

archaeal communities showed a similar clustering pattern suggest potential interactions (*e.g.* synergy, competition) that deserve further investigation.

During the first weeks of biofilm development, the most abundant OTUs belonging to class *Deltaproteobacteria* (OTU-D3 and OTU-D4) were closely related to *Desulfobulbus propionicus*. Interestingly, this species has recently been identified by Sun and coworkers as the main SRB in outer layers of sewer biofilms (10). *D. propionicus* reduces sulfate via the incomplete oxidation of organic acids such as lactate, propionate, butyrate and ethanol to acetate (53), all of them available in the inlet wastewater. In turn, the SRB community in mature biofilms was mainly composed of a deltaproteobacterium closely related to *Desulfobacter postgatei* (OTU-D1), whereas sequences affiliated to SRB colonizers (i.e. OTU-D3 and OTU-D4) were rare after one year of incubation (Fig. S10).

Hydrogenotrophic methanogens (belonging to orders *Methanomicrobiales* or *Methanobacteriales*) may use H_2 generated in fermentative metabolisms or act as hydrogen scavengers in syntrophic growth with acetate-oxidising microorganisms (54–57). Also, acetate produced during fermentation of organic substrates by anaerobic heterotrophs within the biofilm matrix would be used by acetoclastic methanogens (*Methanosarcinaceae* and *Methanosaetaceae*) (58). The identification of sequences belonging to both groups of methanogens (hydrogenotrophic and acetoclastic) in our experimental system during the study period lends support to a progressive change of methanogenic pathways over time in relation to both local environmental conditions and the composition of the archaeal community at each stage of biofilm development.

Methanobrevibacter smithii and *Methanosphaera stadtmanae* (*Methanobacteriales*) are considered to be the prevalent methanogens in the human gut (59). In our study,

Applied and Environmental Microbiology

539 sequences belonging to both species were identified in DGGE fingerprints from inlet
540 wastewater samples and in pyrotag libraries from the first weeks of biofilm
541 development, suggesting that archaeal colonizers at early stages of biofilm development
542 derive from human fecal material in wastewater. These human-derived methanogens
543 were probably outcompeted later on by acetoclastic methanogens (*e.g. Methanosaeta*
544 *concilii*), which would probably be more adapted to environmental conditions in the
545 pilot plant. The time needed by these better-adapted methanogens to get established in
546 the biofilm matrix is consistent with the low CH_4 production during the initial phases of
547 biofilm development. During this first stage, methanogenesis was also probably
548 inhibited by sulfate reducers, which lower the H_2 potential pressure below levels
549 required by methanogens when sulfate is not limiting (60). Despite the well-known
550 competitive interaction between SRB and MA, several studies have demonstrated that
551 both groups coexist under certain conditions (60, 61). Particularly, Struchtemeyer and
552 co-workers reported that low levels of sulfate may favour acetate consumption by MA
553 rather than by SRB (62). In this regard, and although it is always risky to infer
554 functional properties from phylogeny (63), sequences affiliated to both
555 *Deltaproteobacteria* and MA identified in mature biofilms were closely related to
556 species able to use acetate (*i.e. D. postgatei* and *M. concilii,* respectively). Accordingly,
557 the increase in CH_4 production measured after one year of incubation might be
558 explained by the establishment of acetoclastic methanogens in the biofilm favored by a
559 greater availability of acetate in wastewater. Besides, the increase in CH_4 production
560 could also been favored by the stratification of both groups within the biofilm matrix as
561 recently reported (10) although in our case no measurements aimed to resolve the
562 spatial organization of SRB and MA in the studied biofilms were carried out.

563 Altogether, this study provides data that confirm the capacity of our laboratory
564 experimental system to mimic the functioning of full-scale sewers both
565 microbiologically and operationally in terms of H_2S and CH_4 production, and
566 composition of microbial communities during biofilm growth. Whereas H_2S emission
567 was notably high during early stages of biofilm development, CH_4 emissions increased
568 after biofilm maturation coinciding with a establishment of a methanogenic community
569 better adapted to sewer conditions; for that reason, it is important to take into account
570 that the management of sewer systems is really important from the first stages of sewer
571 functioning. Although further research is needed to better resolve the dynamics of the
572 bacterial communities in biofilms and to identify the key bacterial players involved in
573 both nutrient transformations and potential syntrophic interactions that occur in these
574 complex ecosystems, our results should be valuable when designing optimal strategies
575 to mitigate H_2S and CH_4 emissions from sewer systems.

576 **ACKNOWLEDGMENTS**

577 Authors thank the four anonymous reviewers for the useful comments and suggestions
578 made during the review process. This study was partially funded by the Spanish
579 Government Ministerio de Economía y Competitividad through projects GEISTTAR
580 (CTM2011-27163) and ARCOS (CGL2012-33033) and by the European Commission
581 through projects FP7-PEOPLE-2011-CIG303946, 2010-RG277050 and the ITN-Project
582 SANITAS (the REA agreement 289193). Maite Pijuan is a recipient of a Ramon y Cajal
583 research fellowship (RYC-2009-04959) and Olga Auguet benefits from a FI research
584 fellowship (2014FI_B1 00032) from the Catalan Government. ICRA is a recipient of a
585 Consolidated Research Group grant (2014 SGR 291) from the Catalan Government.

586

REFERENCES

1. **Metcalf and Eddy I**. 2003. Wastewater engineering, treatment and reuse. Series in civil and environmental engineering, 4th ed. Tata McGraw-Hill Publishing Company Limited, New Delhi, India.

2. **Hvitved-Jacobsen T**. 2002. Sewer Processes – Microbial and Chemical Process Engineering of Sewer Networks. Boca Raton: CRC Press., 1st ed. CRC Press, Boca Raton, FL.

3. **Dreeszen PH**. 2003. The key to understanding and controlling bacterial growth in Automated Drinking Water Systems, 2nd ed. Edstrom Industries Incorporated, Wisconsin.

4. **Boon A**. 1995. Septicity in sewers: Causes, consequences and containment. Water Sci. Technol. **31**:237–253.

5. **Boon A**. 1998. Avoiding the problems of septic sewage. Water Sci. Technol. **37**:223–231.

6. **Thistlethwayte DKB**. 1972. The Control of Sulfides in Sewerage Systems. Sydney.

7. **Ganigue R, Gutierrez O, Rootsey R, Yuan Z**. 2011. Chemical dosing for sulfide control in Australia: An industry survey. Water Res. **45**:6564–6574.

8. **Guisasola A, de Haas D, Keller J, Yuan Z**. 2008. Methane formation in sewer systems. Water Res. **42**:1421–1430.

9. **Foley J, Yuan Z, Lant P**. 2009. Dissolved methane in rising main sewer systems: field measurements and simple model development for estimating greenhouse gas emissions. Water Sci. Technol. **60**:2963–2971.

10. **Sun J, Hu S, Sharma KR, Ni B-J, Yuan Z**. 2014. Stratified Microbial Structure and Activity in Sulfide- and Methane- Producing Anaerobic Sewer Biofilms. Appl. Environ. Microbiol. **80**:7042–7052.

11. **IPCC**. 2013. Working group I contribuition to the assessment report climate change 2013: The physical science basis: Final Draft Underlying Scientific-Technical Assessment. Cambridge University. Cambridge, U.K. and New York.

12. **Foley J, Yuan Z, Keller J, Senante E, Chandran K, Willis J, Shah A, van Loosdrecht M, van Voorthuizen E**. 2011. N2O and CH4 emission from wastewater collection and treatment systems: state of the science report.

13. **Rodriguez-Caballero A, Aymerich I, Poch M, Pijuan M**. 2014. Evaluation of process conditions triggering emissions of green-house gases from a biological wastewater treatment system. Sci. Total Environ. **493**:384–391.

14. **Auguet O, Pijuan M, Guasch-Balcells H, Borrego CM, Gutierrez O**. 2015. Implications of Downstream Nitrate Dosage in anaerobic sewers to control sulfide and methane emissions. Water Res. **68**:522–532.

15. **Jiang G, Sharma KR, Guisasola A, Keller J, Yuan Z**. 2009. Sulfur transformation in rising main sewers receiving nitrate dosage. Water Res. **43**:4430–4440.

16. **Mohanakrishnan J, Gutierrez O, Sharma KR, Guisasola A, Werner U, Meyer RL, Keller J, Yuan Z**. 2009. Impact of nitrate addition on biofilm properties and activities in rising main sewers. Water Res. **43**:4225–4237.

17. **Mohanakrishnan J, Gutierrez O, Meyer RL, Yuan Z**. 2008. Nitrite effectively inhibits sulfide and methane production in a laboratory scale sewer reactor. Water Res. **42**:3961–3971.

18. **Jiang G, Gutierrez O, Sharma KR, Yuan Z**. 2010. Effects of nitrite concentration and exposure time on sulfide and methane production in sewer systems. Water Res. **44**:4241–4251.

19. **Jiang G, Gutierrez O, Yuan Z**. 2011. The strong biocidal effect of free nitrous acid on anaerobic sewer biofilms. Water Res. **45**:3735–3743.

20. **Firer D, Friedler E, Lahav O**. 2008. Control of sulfide in sewer systems by dosage of iron salts: comparison between theoretical and experimental results, and practical implications. Sci. Total Environ. **392**:145–156.

21. **Gutierrez O, Mohanakrishnan J, Sharma KR, Meyer RL, Keller J, Yuan Z**. 2008. Evaluation of oxygen injection as a means of controlling sulfide production in a sewer system. Water Res. **42**:4549–4561.

22. **Gutierrez O, Park D, Sharma KR, Yuan Z**. 2010. Iron salts dosage for sulfide control in sewers induces chemical phosphorus removal during wastewater treatment. Water Res. **44**:3467–3475.

23. **Gutierrez O, Park D, Sharma KR, Yuan Z**. 2009. Effects of long-term pH elevation on the sulfate-reducing and methanogenic activities of anaerobic sewer biofilms. Water Res. **43**:2549–2557.

24. **Gutierrez O, Sudarjanto G, Ren G, Ganigué R, Jiang G, Yuan Z**. 2014. Assessment of pH shock as a method for controlling sulfide and methane formation in pressure main sewer systems. Water Res. **48**:569–578.

25. **Lovley DR, Klug MJ**. 1983. Sulfate Reducers Can Outcompete Methanogens at Freshwater Sulfate Concentrations. Appl. Environ. Microbiol. **45**:187–192.

26. **Omil F, Lens P, Visser A, Hulshoff Pol LW, Lettinga G**. 1998. Long-term competition between sulfate reducing and methanogenic bacteria in UASB reactors treating volatile fatty acids. Biotechnol. Bioeng. **57**:676–685.

27. **Gutierrez O, Sudarjanto G, Sharma KR, Keller J, Yuan Z**. 2011. SCORe-CT: a new method for testing effectiveness of sulfide-control chemicals used in sewer systems. Water Sci. Technol. **64**:2381–2388.

28. **Gutierrez O, Sutherland-Stacey L, Yuan Z**. 2010. Simultaneous online measurement of sulfide and nitrate in sewers for nitrate dosage optimisation. Water Sci. Technol. **61**:651–658.

29. **Keller-Lehmann B, Corrie S, Ravn R**. 2006. Preservation and simultaneous analysis of relevant soluble sulfur species in sewage samplesSecond International IWA Conference on Sewer Operation and Maintenance.

30. **APHA**. 1998. Standard Methods for the Examination of Water and Wastewater, 21st ed. American Public Health Administration, Washington, DC.

31. **Muyzer G, de Waal EC, Uitterlinden AG**. 1993. Profiling of complex microbial populations by denaturing gradient gel electrophoresis analysis of polymerase chain reaction-amplified genes coding for 16S rRNA. Appl. Environ. Microbiol. **59**:695–700.

32. **Muyzer G, Ramsing NB**. 1995. Molecular methods to study the organization of microbial communities. Water Sci Technol **32**:1–9.

33. **Lane DJ**. 1991. 16S/23S rRNA sequencing, p. 115–175. *In* Stackebrandt, E., Goodfellow, M (ed.), Nucleic acid techniques in bacterial systematics. John Wiley and Sons, New York.

34. **Llirós M, Casamayor EO, Borrego C**. 2008. High archaeal richness in the water column of a freshwater sulfurous karstic lake along an interannual study. FEMS Microbiol. Ecol. **66**:331–342.

35. **Edgar RC, Haas BJ, Clemente JC, Quince C, Knight R**. 2011. UCHIME improves sensitivity and speed of chimera detection. Bioinformatics **27**:2194–2200.

36. **Hall T**. 1999. BioEdit: a user-friendly biological sequence alignment editor and analysis program for Windows 95/98/NT. Nucleic Acids Symp Ser **41**:95–98.

37. **Altschul SF, Gish W, Miller W, Myers EW, Lipman DJ**. 1990. Basic local alignment search tool. J. Mol. Biol **215**:403–410.

38. **Maeda H, Fujimoto C, Haruki Y, Maeda T, Kokeguchi S, Petelin M, Arai H, Tanimoto I, Nishimura F, Takashiba S**. 2003. Quantitative real-time PCR using TaqMan and SYBR Green for Actinobacillus actinomycetemcomitans , Porphyromonas gingivalis , Prevotella intermedia , tetQ gene and total bacteria. FEMS Immunol. Med. Microbiol. **39**:81–86.

39. **Takai K, Horikoshi K**. 2000. Rapid Detection and Quantification of Members of the Archaeal Community by Quantitative PCR Using Fluorogenic Probes Rapid Detection and Quantification of Members of the Archaeal Community by Quantitative PCR Using Fluorogenic Probes. Appl. Environ. Microbiol. **66**:5066–5072.

40. **Stahl D, Amman**. 1991. Development and application of nucleic acid probes, p. 205–248. *In* E. Stackebrandt and M. Goodfellow (ed.), Nucleic acid techniques in bacterial systematics. John Wiley & Sons, New York.

41. **Ben-Dov E, Brenner A, Kushmaro A**. 2007. Quantification of sulfate-reducing bacteria in industrial wastewater, by real-time polymerase chain reaction (PCR) using dsrA and apsA genes. Microb. Ecol. **54**:439–451.

42. **Bustin S a, Benes V, Garson J a, Hellemans J, Huggett J, Kubista M, Mueller R, Nolan T, Pfaffl MW, Shipley GL, Vandesompele J, Wittwer CT**. 2009. The MIQE guidelines: minimum information for publication of quantitative real-time PCR experiments. Clin. Chem. **55**:611–622.

43. **Øvreås L, Forney L, Daae FL, Torsvik V**. 1997. Distribution of bacterioplankton in meromictic lake Saelenvannet, as determined by denaturing gradient gel

electrophoresis of PCR-amplified gene fragments coding for 16S rRNA. Appl. Environ. Microbiol. **63**:3367–3373.

44. **DeLong EF**. 1992. Archaea in coastal marine environments. Proc. Natl. Acad. Sci. U. S. A. **89**:5685–5689.

45. **Dowd SE, Callaway TR, Wolcott RD, Sun Y, McKeehan T, Hagevoort RG, Edrington TS**. 2008. Evaluation of the bacterial diversity in the feces of cattle using 16S rDNA bacterial tag-encoded FLX amplicon pyrosequencing (bTEFAP). BMC Microbiol **8**:125-132.

46. **Schloss PD, Westcott SL, Ryabin T, Hall JR, Hartmann M, Hollister EB, Lesniewski R a, Oakley BB, Parks DH, Robinson CJ, Sahl JW, Stres B, Thallinger GG, Van Horn DJ, Weber CF**. 2009. Introducing mothur: open-source, platform-independent, community-supported software for describing and comparing microbial communities. Appl. Environ. Microbiol. **75**:7537–7541.

47. **Lozupone C, Knight R**. 2005. UniFrac: a new phylogenetic method for comparing microbial communities. Appl. Environ. Microbiol. **71**:8228–8235.

48. **Tamura K, Peterson D, Peterson N, Stecher G, Nei M, Kumar S**. 2011. MEGA5: Molecular evolutionary genetics analysis using maximum likelihood, evolutionary distance, and maximum parsimony methods. Mol. Biol. Evol. **28**:2731–2739.

49. **Jabari L, Gannoun H, Cayol J-L, Hedi A, Sakamoto M, Falsen E, Ohkuma M, Hamdi M, Fauque G, Ollivier B, Fardeau M-L**. 2012. *Macellibacteroides fermentans* gen. nov., sp. nov., a member of the family *Porphyromonadaceae*

isolated from an upflow anaerobic filter treating abattoir wastewaters. Int. J. Syst. Evol. Microbiol. **62**:2522–2527.

50. **Kaneuchi C, Mitsuoka T**. 1978. Bacteroides microfusus, a New Species from the Intestines of Calves, Chickens, and Japanese Quails. Int. J. Syst. Bacteriol. **28**:478–481.

51. **Oremland RS, Polcin S**. 1982. Methanogenesis and sulfate reduction: competitive and noncompetitive substrates in estuarine sediments. Appl. Environ. Microbiol. **44**:1270–1276.

52. **Kisand V, Wikner J**. 2003. Limited resolution of 16S rDNA DGGE caused by melting properties and closely related DNA sequences. J. Microbiol. Methods **54**:183–191.

53. **Holmes DE, Bond DR, Lovley DR**. 2004. Electron Transfer by Desulfobulbus propionicus to Fe(III) and Graphite Electrodes. Appl. Environ. Microbiol. **70**:1234–1237.

54. **Hattori S, Kamagata Y, Hanada S, Shoun H**. 2000. *Thermacetogenium phaeum* gen. nov., sp. nov., a strictly anaerobic, thermophilic, syntrophic acetate-oxidizing bacterium. Int. J. Syst. Evol. Microbiol. **50**:1601–1609.

55. **Petersen SP, Ahring BK**. 1991. Acetate oxidation in a thermophilic anaerobic sewage-sludge digestor: the importance of non-aceticlastic methanogenesis from acetate. FEMS Microbiol. Lett. **86**:149–152.

752 56. **Schnürer A, Svensson BH, Schink B**. 1997. Enzyme activities in and energetics
753 of acetate metabolism by the mesophilic syntrophically acetate-oxidizing anaerobe.
754 FEMS Microbiol. Lett. **154**:331–336.

755 57. **Karakashev D, Batstone DJ, Trably E, Angelidaki I**. 2006. Acetate oxidation is
756 the dominant methanogenic pathway from acetate in the absence of
757 *Methanosaetaceae*. Appl. Environ. Microbiol. **72**:5138–5141.

758 58. **Ferry JG**. 1992. Methane from Acetate. J. Bacteriol. **174**:5489–5495.

759 59. **Dridi B, Henry M, El Khéchine A, Raoult D, Drancourt M**. 2009. High
760 prevalence of *Methanobrevibacter smithii* and *Methanosphaera stadtmanae*
761 detected in the human gut using an improved DNA detection protocol. PLoS One
762 **4**:e7063.

763 60. **Lovley DR, Dwyer DF, Klug MJ**. 1982. Kinetic analysis of competition between
764 sulfate reducers and methanogens for hydrogen in sediments. Appl. Environ.
765 Microbiol. **43**:1373–1379.

766 61. **Kristjansson JK, Schönheit P, Thauer RK**. 1982. Different Ks values for
767 hydrogen of methanogenic bacteria and sulfate reducing bacteria: An explanation
768 for the apparent inhibition of methanogenesis by sulfate. Arch. Microbiol. **131**:278–
769 282.

770 62. **Struchtemeyer CG, Elshahed MS, Duncan KE, McInerney MJ**. 2005. Evidence
771 for aceticlastic methanogenesis in the presence of sulfate in a gas condensate-
772 contaminated aquifer. Appl. Environ. Microbiol. **71**:5348–5353.

773 63. **Gray ND, Head IM**. 2001. Linking genetic identity and function in communities
774 of uncultured bacteria. Environ. Microbiol. **3**:481–492.

775

776

Captions to Figures

Figure 1. (A) Temporal changes of microbial biomass in reactors R1, R2 and R3. (B) Sulfide production rates determined in the batch tests on reactors R1, R2 and R3 and sulfate concentration in inlet wastewater (IW, grey area).

Figure 2. Negative images of DGGE gels of 16S rRNA gene fingerprints for Bacteria (A) and Archaea (B) from wastewater and biofilms grown in R1. Hierarchical clustering of samples based on Dice similarity indexes of the banding patterns are also shown. White arrows indicate biofilm samples used in further pyrosequencing analyses (Weeks 1, 5 and 13).

Figure 3. Relative abundance of sequences (%) affiliated to (A) main bacterial classes and (B) main archaeal genera in week 1, week 5, week 13, One Year and full-scale sewer biofilm samples.

Figure 4. Bubble plots of bacterial (A) and archaeal (B) OTUs showing their relative abundances across samples, their taxonomy affiliation (at Genus level) and the percentage identity to the first BLAST hit against reference sequence databases. Data values are proportional to radius and plotted in a logarithmic scale as indicated below the graph. Relative abundance (%) of each OTU at different sampling points is indicated next to the corresponding bubble (grey figures).

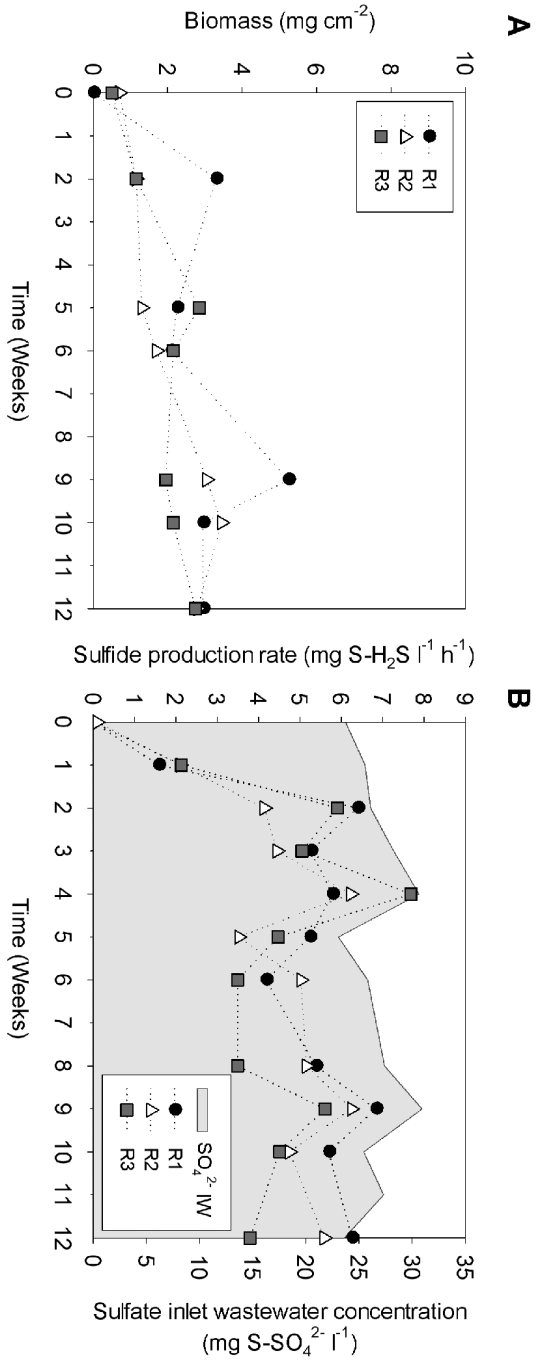

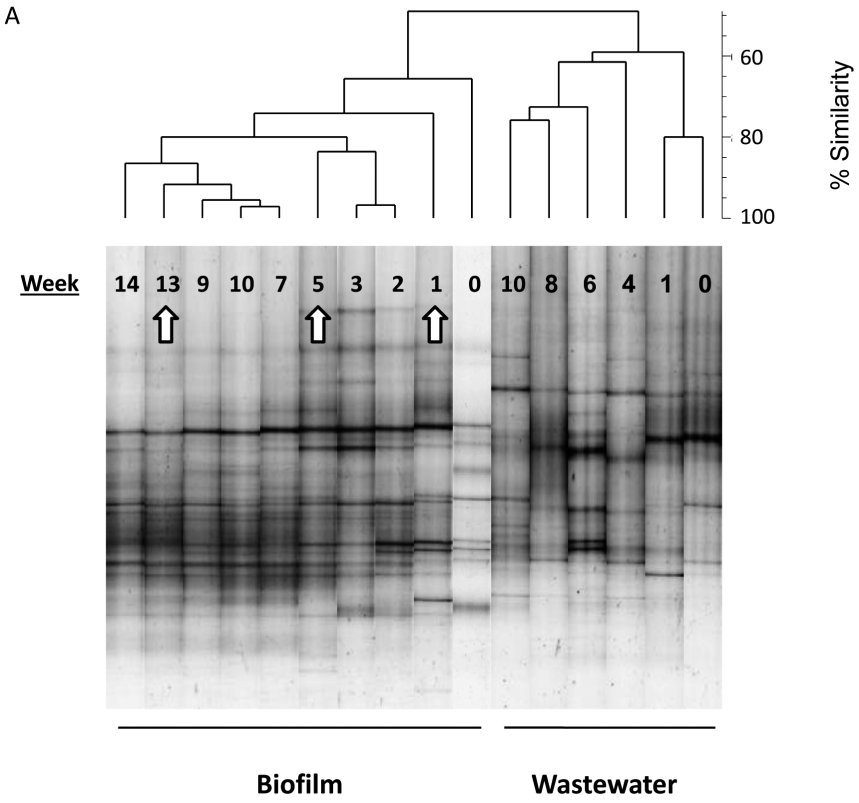

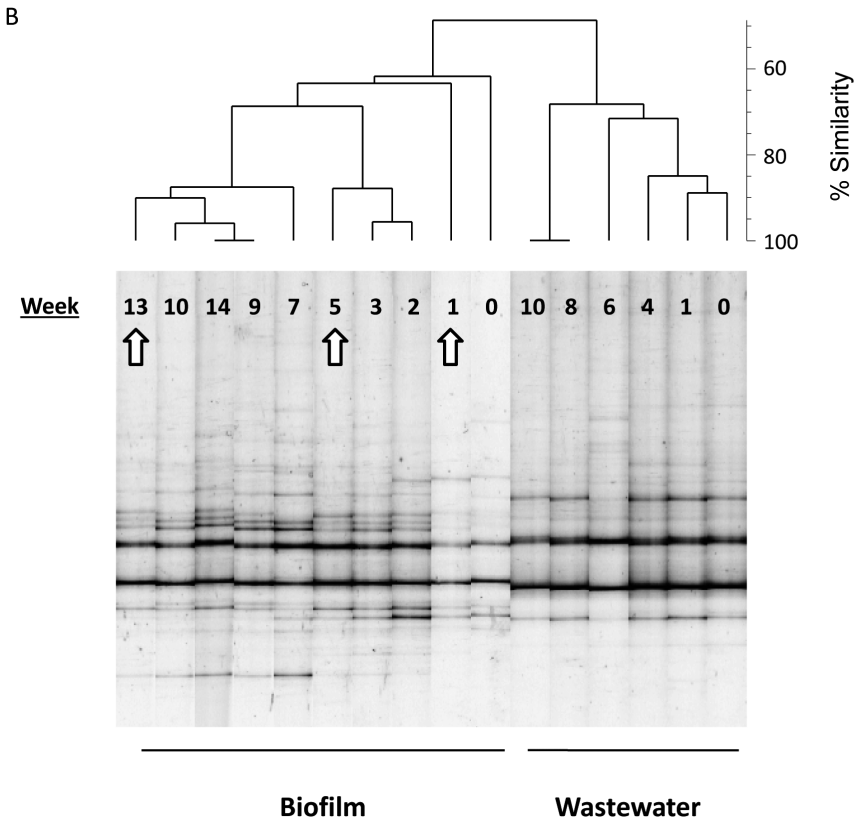

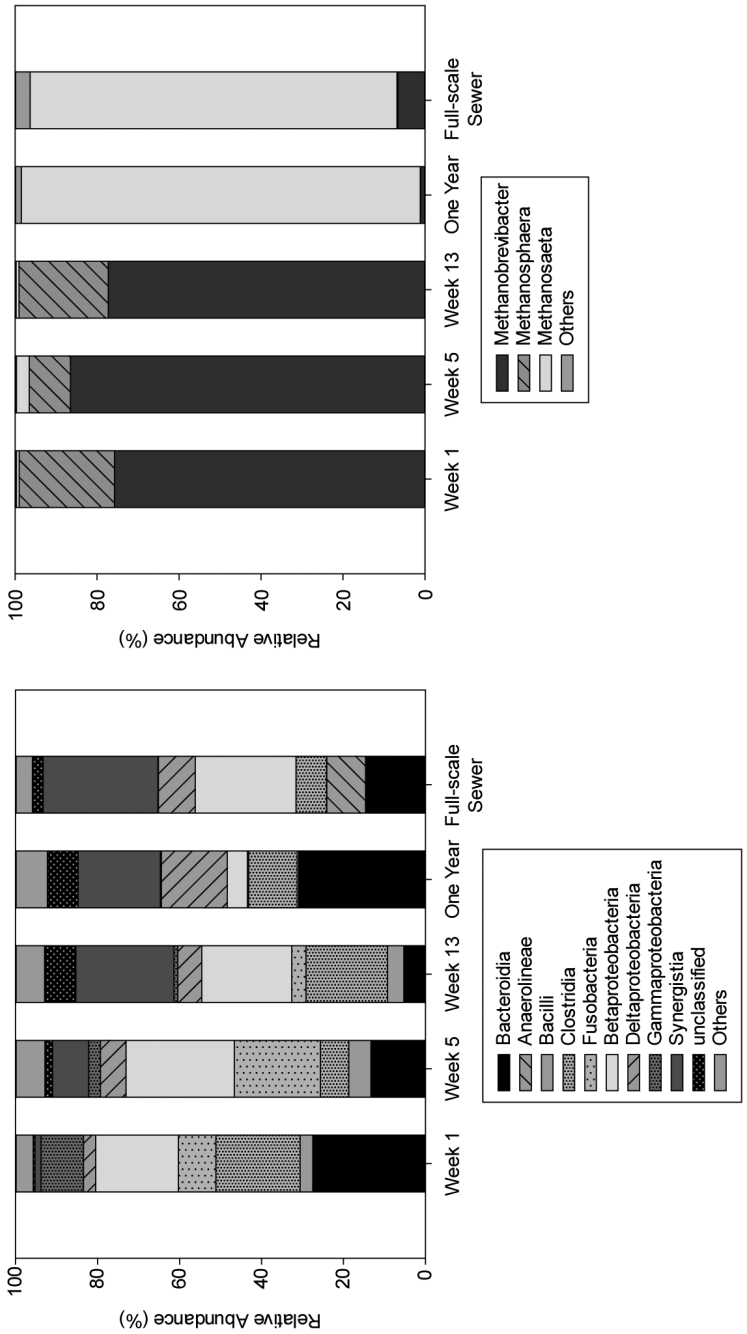

A

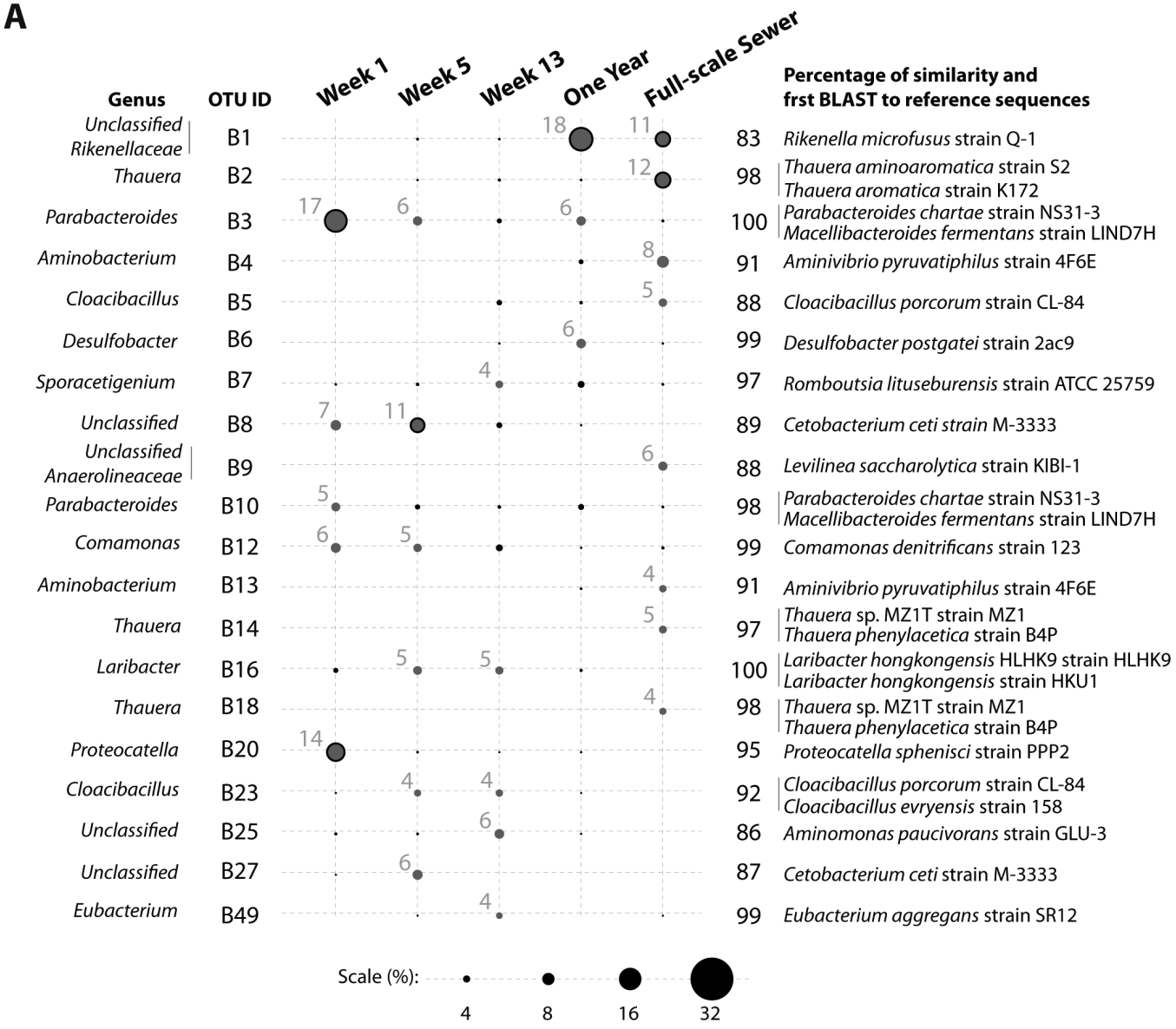

B